

See discussions, stats, and author profiles for this publication at: <https://www.researchgate.net/publication/227707280>

Rheological Behaviors and Miscibility of Mixture Solution of Polyaniline and Cellulose Dissolved in an Aqueous System

ARTICLE in BIOMACROMOLECULES · JUNE 2012

Impact Factor: 5.75 · DOI: 10.1021/bm3006243 · Source: PubMed

CITATIONS

16

READS

44

7 AUTHORS, INCLUDING:



Xingwei Shi

Harbin Engineering University

12 PUBLICATIONS 75 CITATIONS

SEE PROFILE



Ang Lu

Wuhan University

40 PUBLICATIONS 455 CITATIONS

SEE PROFILE



Lina Zhang

Fourth Military Medical University

493 PUBLICATIONS 12,584 CITATIONS

SEE PROFILE



Ji Li

Hong Kong Baptist University

103 PUBLICATIONS 1,345 CITATIONS

SEE PROFILE

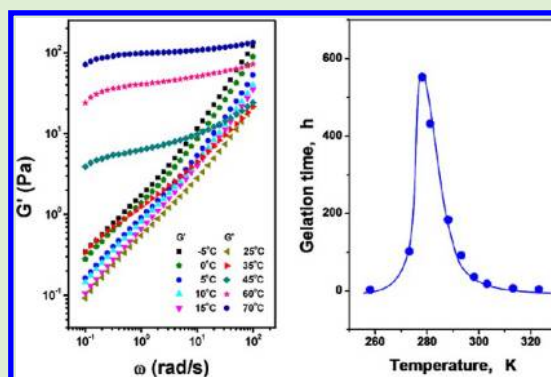
Rheological Behaviors and Miscibility of Mixture Solution of Polyaniline and Cellulose Dissolved in an Aqueous System

Xingwei Shi,[†] Ang Lu,[†] Jie Cai,[†] Lina Zhang,^{*,†} Hongming Zhang,[‡] Ji Li,[‡] and Xianhong Wang[‡]

[†]Department of Chemistry, Wuhan University, 430072, China

[‡]Key Lab of Polymer Ecomaterials, Changchun Institute of Applied Chemistry, Chinese Academy of Sciences, 130022, China

ABSTRACT: In our previous work, supramolecular films composed of hydrophilic cellulose and hydrophobic polyaniline (PANI) dissolved in NaOH/urea aqueous solution at low temperature through rearrangement of hydrogen bonds have been constructed. To further understand the miscibility and processability of the complex solution, the dynamic rheological behaviors of the PANI/cellulose complex solution were investigated, for the first time, in the present work. Transmission electron microscope (TEM) results demonstrated that the inclusion complexes consisted of PANI and cellulose, existed in the aqueous solution, showing a good miscibility. Time–temperatures superposition (tTs) results indicated that the PANI/cellulose solution exhibited a homogeneous system, and the complex solution was more stable than the cellulose solution in the temperature range from 5 to 25 °C. Winter–Chambon theory was proved to be capable of describing the gelation behavior of the PANI/cellulose complex solution. The relaxation exponent at the gel point was calculated to be 0.74, lower than the cellulose solution, indicating strong interactions between PANI and cellulose chains. Relatively larger flow activation energy of the PANI/cellulose solution suggested the formation and rupture of linkages in “junction zones” during the gelation processes. Furthermore, PANI/cellulose gels could form at elevated temperature as a result of the physical cross-linking and chain entanglement, and it was a thermoirreversible process. Moreover, the PANI/cellulose solution remained a liquid state for a long time at the temperature range from 0 to 8 °C, which is important for the industry process.



INTRODUCTION

Polyaniline (PANI) is an unique and important conducting polymer because of its controllable chemical and physical properties, which depend on its oxidation and protonation states.^{1–6} However, it is difficult to dissolve PANI in common solvents, which limits its applications. In our previous work, PANI doped with acidic phosphate ester has been dissolved in the cellulose/NaOH/urea aqueous solution at low temperature, giving a dark green and transparent complex film.⁷ In the mixture solution, water-soluble cellulose inclusion complexes (ICs) were entangled by PANI through hydrogen bonds between the –NH and –OH groups to form supramolecular complexes, leading to the dissolution of PANI in the aqueous solution. Moreover, the complex solution displays a homogeneous phase, suggesting that the mixture system has good miscibility between the stiff macromolecules of PANI and cellulose. Therefore, a basic understanding of the solution properties and rheology behavior of the PANI/cellulose complex solution is necessary for designing and fabricating new PANI-based supramolecular materials with advanced properties.^{8–11}

Dynamics rheological techniques have attracted strong interest as a powerful approach to study the supramolecular system. Moreover, microstructures and interactions of the supramolecular system or multiphase polymer solutions have

been investigated in complex systems.^{12–17} With the help of rheometry, the microstructure and the rheological properties of thermoreversible nanoparticle gels, the microstructure and dynamics of colloidal silica and polymer in a mixed solvent, interactions and structure of wormlike micelles and nanoparticles in aqueous stock solution, and interactions between polymer and synthetic clay in aqueous solution, as well as hydrogen bonding interactions in miscible polymer blends, have been successfully investigated.^{18–22} Linear dynamic viscoelasticity of miscible polymer blend systems with specific interaction (intermolecular hydrogen bonding) can answer the fundamental questions such as miscibility of polymer blends with intermolecular hydrogen bonding.²³

In this article, the intermolecular interactions, rheological properties, and the gelation behaviors of PANI/cellulose in the 7 wt % NaOH/12 wt % urea aqueous solution with different temperatures and concentrations were investigated. The complex structure and the miscibility of PANI and cellulose in aqueous solution were also analyzed to clarify the interactions between the PANI and cellulose. The understanding of the supramolecular complexes composed of

Received: April 22, 2012

Revised: June 18, 2012

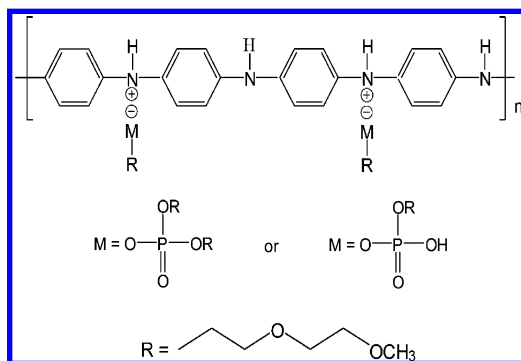
Published: June 20, 2012

hydrophobic and hydrophilic polymers in aqueous solution should be important to both the scientific and the industrial community.

EXPERIMENTAL SECTION

Materials. Cellulose (the cotton linter pulp) with an α -cellulose content of more than 95% was supplied by Hubei Chemical Fiber Co. Ltd. (Xiangfan, China). Its weight-average molecular weight (M_w) was determined by laser light scattering in a 4.6 wt % LiOH/15.0 wt % urea aqueous solution to be 9.8×10^4 .²⁴ NaOH and urea of analytical grade (Shanghai Chemical Reagent Co. Ltd. China) were used without further purification. The cellulose sample was dried under vacuum at 55 °C for 24 h to remove any moisture before use. Polyaniline (PANI)

Scheme 1. Chemical Structure of Polyaniline Doped with Acidic Phosphate Ester (M)^{25,26}



doped with acidic phosphate ester (Scheme 1) aqueous solution was supplied by Changchun Institute of Applied Chemistry (Chinese Academy of Sciences, China). Its M_w value was determined in *N*-methyl-2-pyrrolidone (NMP) solvent with laser light scattering to be 3.0×10^4 .^{25,26}

Solution Preparation. A mixture solution with NaOH/urea/ H_2O ratio of 7:12:81 by weight was precooled to -12 °C. A total of 4.2 g cellulose was immediately dispersed into the solvent system (100 g) under vigorous stirring for 4 min to obtain a transparent cellulose solution. Subsequently, PANI doped with acidic phosphate ester (4.2%, w/v) precooled to 0 °C was immediately dropped into the cellulose solution under vigorous stirring for 3 min at ambient temperature to form a blue PANI/cellulose solution and then was subjected to centrifuge to degas at 7200 rpm for 20 min at 8 °C. The content of PANI and cellulose in mixture solution was varied by adjusting the ratio of the cellulose solution and PANI solution and summarized in Table 1.

Table 1. Components of PANI/Cellulose Solution in the NaOH/Urea Aqueous System

PANI content in mixture	solid content in the aqueous solution	
	cellulose (wt%)	PANI (wt%)
P4	3.8	0.16
P8	3.6	0.32
P15	3.4	0.60
P25	3.0	0.74

Characterization. Transmission electron microscopy (TEM) observation of the molecular morphology of the dried sample from the P15 solution (0.6 wt % PANI/3.4 wt % cellulose, Table 1) was carried out on a JEM-2010 (HT) transmission electron microscope (JEOL TEM Japan). The P15 solution was diluted by 7 wt % NaOH/12 wt % urea aqueous solution, and then a thin layer of the dilute PANI/cellulose aqueous solution was suspended on a holey carbon

film, which was supported on a copper grid. The specimen was dried in air at ambient temperature, and then imaged on TEM at an accelerating voltage of 200 KV.

Dynamic rheological measurements were carried out on an ARES RFSIII rheometer (TA Instruments, U.S.A.). A double-concentric cylinder Couette with a gap of 2 mm was used to measure dynamic viscoelastic parameters such as shear storage modulus (G') and loss modulus (G'') as functions of angular frequency (ω), temperature (T), or time (t). The rheometer was equipped with two force transducers allowing torque measurements in the range from 0.004 to 1000 g·cm. The values of the strain amplitude were checked to ensure that all measurements were set as 10%, which was within a linear viscoelastic regime. For each measurement, a fresh PANI/cellulose solution was prepared, and then the degassed PANI/cellulose solution was poured into the Couette geometry instrument, which had been kept at each measurement temperature without preshearing or oscillating. Temperature control was established by connection with a Julabo FS18 cooling/heating bath kept within ± 0.2 °C of the desired temperature over an extended period of time. To prevent dehydration during rheological measurements, a thin layer of low viscosity paraffin oil was spread on the exposed surface of the measured solution. For the frequency and time sweep measurements, $t = 0$ min was defined when the temperature reached the desired value. The sweep of the frequency was from 0.1 to 100 rad/s. The gelation kinetics was studied at constant temperature as a function of time at $\omega = 1$ rad/s. The dynamic temperature sweep measurements were conducted from 0 to 60 °C at $\omega = 1$ rad/s and with a heating or cooling rate of 2 °C/min.

RESULTS AND DISCUSSION

Miscibility and Supramolecular Structure of PANI/Cellulose Solution. Figure 1 shows the photographs of the

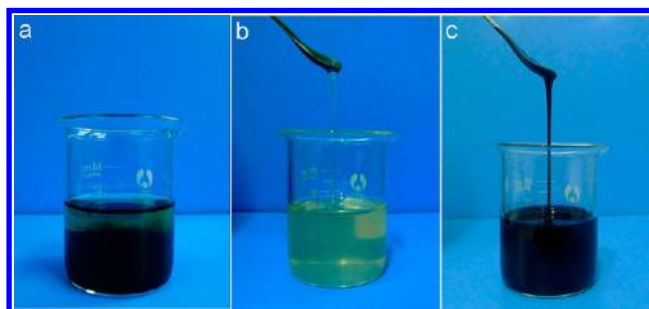


Figure 1. Photographs of PANI suspensions (a), cellulose solution (b), and PANI/cellulose solution (c).

PANI doped with acidic phosphate ester aqueous solution, cellulose/NaOH/urea aqueous solution, and PANI/cellulose/NaOH/urea aqueous solution, respectively. Clearly, the doped PANI was in a suspension state. In contrast, the PANI/cellulose/NaOH/urea aqueous solution was a homogeneous and dark blue solution, and inherits the viscous character of the cellulose/NaOH/urea aqueous solution. This phenomenon indicated that a complex structure occurred between PANI and cellulose in the solution, leading to the dissolution of PANI. It has been confirmed that NaOH hydrates in the NaOH/urea aqueous solution can be more easily attracted to the cellulose chains through the formation of hydrogen-bonded networks at low temperature, whereas urea could associate with NaOH hydrate to self-assemble on the surface of the NaOH hydrogen-bonded cellulose to form inclusion complexes (ICs), resulting in a water-soluble cellulose IC.²⁷ Figure 2 shows the TEM images of the PANI doped with acidic phosphate ester aqueous suspension, cellulose/NaOH/urea aqueous solution, and PANI/cellulose/NaOH/urea aqueous solution (P15, 0.6 wt % PANI/3.4 wt % cellulose), respectively. The PANI doped with

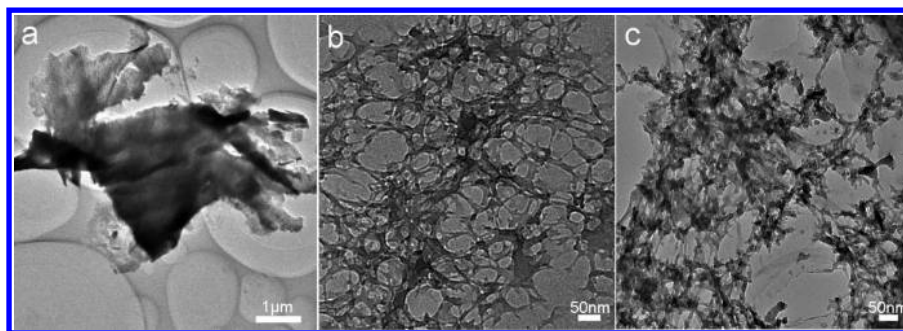


Figure 2. TEM images of the PANI suspensions (a), cellulose solution (b), and PANI/cellulose solution of P15 (c).

acidic phosphate ester was easily to form aggregates with several μm in size (Figure 2a). In our laboratory, it has been proven that the TEM images of the cellulose dilute solution dried at room temperature displays a worm-like pattern of the cellulose IC, and the ICs linked with each other, forming longer, parallel and overcrossed aggregates as a result of the partial dissociation of the ICs.²⁷ From the analysis of TEM images of cellulose dilute solution and PANI/cellulose/NaOH/urea complex solution (Figure 2b,c), similar phenomena were observed, and the average diameter of the IC complex was determined to be, respectively, 9 and 12 nm. Moreover, calculation from the chemical structure for cellulose/NaOH/urea complex and PANI/cellulose/NaOH/urea IC complex gave the values of 5.3 and 6 nm, respectively. These observations, together with the results from the laser light scattering and synchrotron radiation X-ray diffraction in our previous work,^{7,27} and the calculation from their chemical structure, were in good agreement. Namely, the water-soluble cellulose ICs surrounded by urea have been entangled by PANI through intermolecular hydrogen bonds, leading to the homogeneous solution consist with PANI and cellulose. Therefore, PANI and cellulose macromolecules formed supra-molecular complexes in the aqueous solution at low temperature.

Effects of PANI on the Stability of the PANI/Cellulose Solution. The rheological study was an important technique to evaluate the gelation behavior of polymer solutions, as gelation involves a transition from a viscous fluid to a gel. According to the Winter–Chambon criterion, an experimentally established scaling law is applicable to describe the liquidlike terminal behavior:^{28,29}

$$G'(\omega) \propto \omega^2 \quad G''(\omega) \propto \omega \quad (1)$$

$$G''(\omega)/G'(\omega) = \tan \delta = \tan(n\pi/2) \quad (2)$$

where $\tan \delta$ is the loss tangent and n is the relaxation exponent at the gel point. The G' and G'' at various temperatures as a function of the ω for P8 PANI/cellulose solution (0.32 wt % PANI/3.6 wt % cellulose aqueous solution, Table 1) are shown in Figure 3. The typical characteristics of the G' curves can be divided into three segments: a slight flat site with $G' \sim \omega$ at -5°C ; a $G' \sim \omega$ curve with the slope of 1 at 0°C ; and a plateau of the $G' \sim \omega$ curves that became clear as the temperature was raised from 25 to 70°C . Starting from -5 to 0°C , the G' values decreased with elevation of temperature, suggesting that more entanglements between the polyaniline and cellulose chains in the solution at lower temperature. In the range from 0 to 25°C , the PANI/cellulose solutions exhibited liquidlike behavior with G' scaling approximately with $G' \sim \omega$ in the low frequency

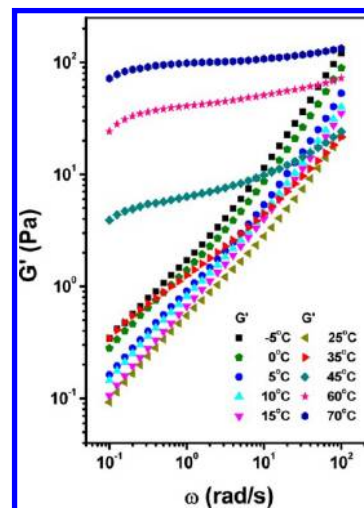


Figure 3. G' as a function of ω at various temperatures of the P8 PANI/cellulose solution.

range, but the terminal behavior ($G' \sim \omega^2$) for a Newtonian fluid was not observed.³⁰ When the temperature was higher than 25°C , the G' curves presented a plateau-like behavior at low frequencies, and its height increased and the width expanded with an increase of temperature. Interestingly, the G' values increased rapidly in the range from 45 to 70°C and showed significantly frequency-independent plateaus at 70°C in the frequency range from 0.1 to 10 rad/s, indicating the existence of a stable structure of the gel network. Within this temperature range, the $G' \sim \omega$ plateau revealed the formation of gel networks between the PANI/cellulose complexes. The likely explanation was that both the PANI/cellulose complex structure and the cellulose IC were destroyed partly at higher temperatures, leading to the physical cross-linking and entanglement of the PANI and cellulose chains. A similar phenomenon has been observed in the cellulose solution, that is, the elastic behaviors of the cellulose solution occurred at high temperature because the junctions between cellulose chains have formed as a result of the self-association of cellulose, leading to the formation of networks.³¹ Therefore, the dynamic rheological properties of the PANI/cellulose solution were similar to that of the cellulose solution, indicating the homogeneous nature of the PANI/cellulose solution.

Typically, a_T is a frequency-scale shift factor required to allow the superposition of the viscoelastic data at temperature T with the data at the reference temperature (T_0). The dependence of a_T with T_0 can be described by the Williams–Landel–Ferry (WLF) equation:^{32,33}

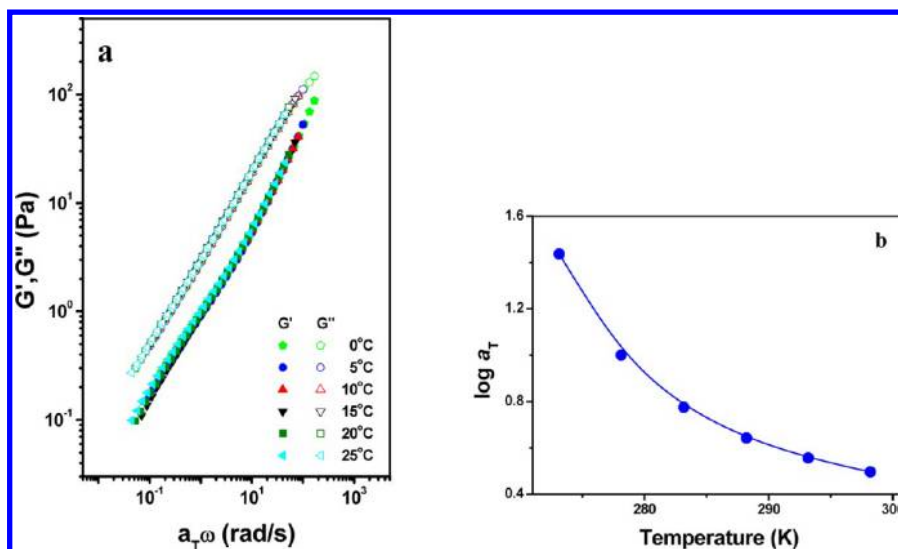


Figure 4. Master curves of G' and G'' for the P8 PANI/cellulose solution as a function of ω at different temperatures (a), and the temperature dependence of the frequency scale shift factor (a_T), at the reference temperature of 5 °C (b).

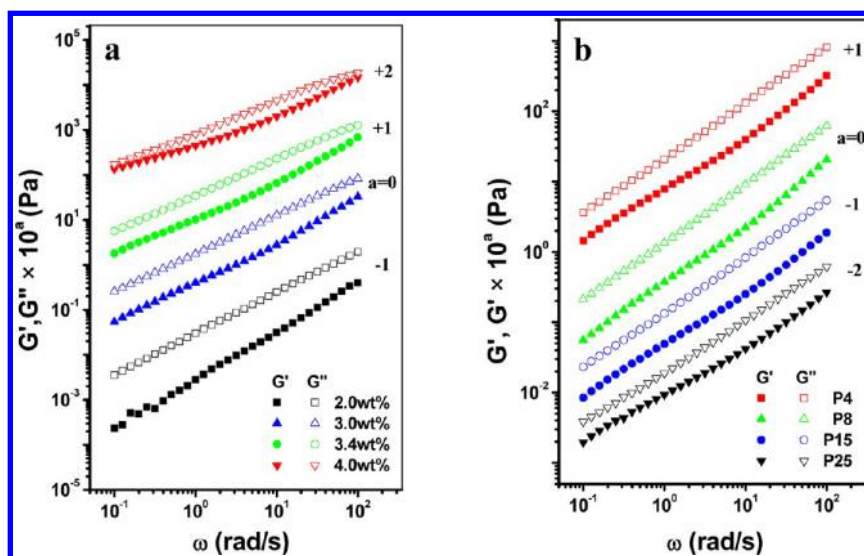


Figure 5. G' and G'' as a function of ω for PANI/cellulose solutions of different concentrations: (a) PANI concentration is 0.6 wt % with the cellulose concentration varied from 2.0 to 4.0 wt %, and (b) P4, P8, P15, and P25 PANI/cellulose solutions. The data are shifted along the vertical axis by 10^n to avoid overlapping.

$$\log a_T = -c_1(T - T_0)/(c_2 + T - T_0) \quad (3)$$

with constants $c_1 = 0.73$ and $c_2 = 28.13$. Here, we show the master curves of PANI/cellulose systems with a reference temperature of 5 °C, as shown in Figure 4. The relation of $\log G'$ and $\log a_T \omega$ for the PANI/cellulose solution exhibited temperature independence, indicating that time–temperature superposition (tTS) matched well for G' and G'' in the terminal region in the range from 0 to 25 °C. From the slopes of the G' and G'' curves, we further obtained the exponent n of $G \sim \omega$ in the terminal region, which depends on the linear viscoelastic behavior of the polymer solutions.^{34,35} The slopes were less than 2 in the terminal region, indicating the presence of hydrogen bonding in PANI/cellulose solution, similar to the poly(vinylphenol)-based miscible blends investigated by Han et al.²³ In our previous work, tTS failed for the 3.9 wt % cellulose in NaOH/thiourea aqueous solution, in which significant deviations were observed in the terminal region in the

temperature range from 5 to 25 °C.³⁶ This suggested that PANI/cellulose solution was more miscible and homogeneous than the pure cellulose solution. However, the tTS failed for the PANI/cellulose solution at a temperature over 25 °C, because deviations in the terminal region for the P8 (Table 1) PANI/cellulose system occurred. It could be contributed by the formation of thermorheological complexes,³⁰ suggesting an onset of the gel network in PANI/cellulose complex system at higher temperature.

Figure 5 shows the G' and G'' curves of the PANI/cellulose solutions as a function of angular frequency at 25 °C. In Figure 5a, the PANI concentration was constantly 0.6 wt % with increasing cellulose concentrations from 2 to 4 wt %. As the cellulose concentration was lower than 3.4 wt %, the supramolecular complex solution exhibited a G' value far smaller than that of G'' at all frequencies and both were strongly dependent on the frequency, indicating a liquid-like behavior. As the cellulose concentration reached 4.0 wt %, the values of

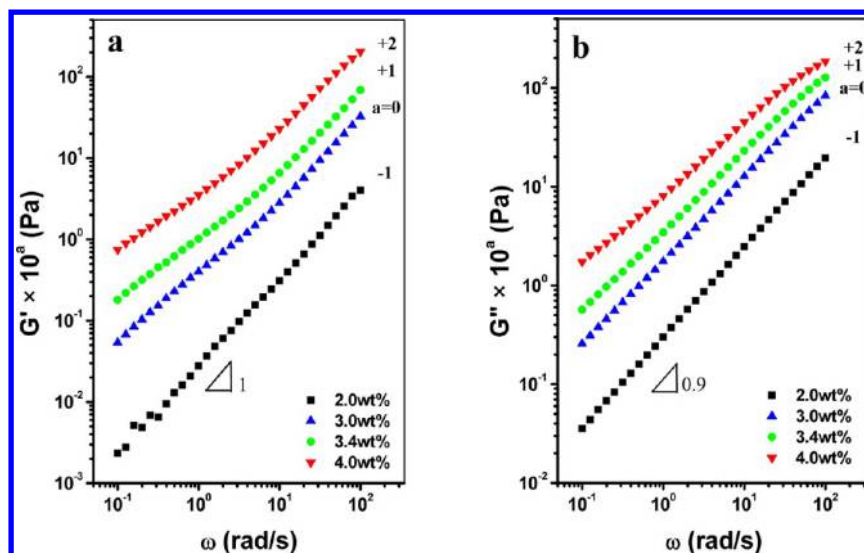


Figure 6. G' (a) and G'' (b) of the 0.6 wt % PANI/cellulose with concentrations from 2 to 4 wt % solutions as a function of ω at 25 °C. The data are shifted along the vertical axis by 10^a to avoid overlapping.

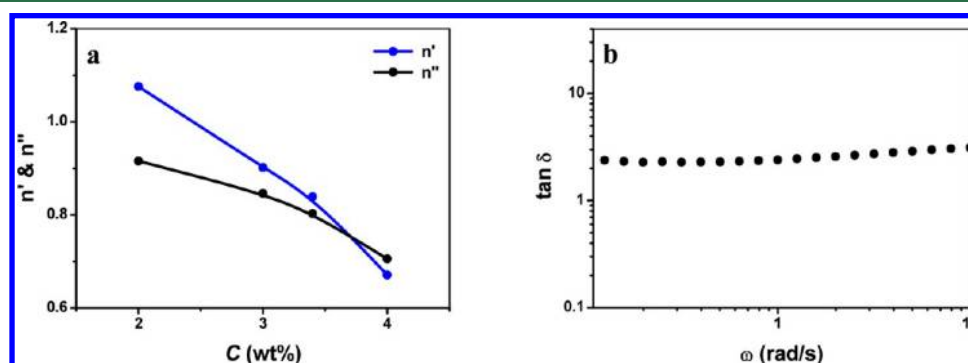


Figure 7. Concentration dependence of exponents n' and n'' obtained from fitting the frequency dependence data of G' and G'' for the 0.6 wt % PANI/cellulose with concentrations from 2 to 4 wt % solutions at 25 °C (a), and $\tan \delta$ as a function of ω for the 0.6 wt % PANI/3.8 wt % cellulose solution (b).

G' was gradually getting close to G'' in the terminal region. The results revealed that, with an increase of the cellulose concentration, the differences between G' and G'' became smaller, which was an evidence of aggregation and entanglement of the IC chains. This indicated that the cellulose concentration and cellulose self-association were dominant factors in the gel formation. In Figure 5b, all G' and G'' curves increased with an increase of frequency, and the G'' values were larger than G' in the entire frequency range measured for various components (Table 1). The explanation for the above observation was that the maximum cellulose concentration in PANI/cellulose solution was below 4 wt % in Figure 5b. Thus, with an increase of the PANI content, the rheological properties of the PANI/cellulose hardly changed. This further demonstrated that the gel formation was dominated by the cellulose concentration. In view of the above results, it can be concluded that PANI played an important role in the improvement on the stability of the cellulose solution in the NaOH/urea aqueous system.

Gelation Behavior of the PANI/Cellulose Solution.

Figure 6 shows the G' and G'' of the PANI/cellulose of $G'(\omega)$ versus ω on the log–log scale varied from 1 to near 0, whereas the slope of the $G''(\omega)$ versus ω varied solution at 25 °C, in which the PANI concentration was constantly 0.6 wt %. The

slope from 0.9 to near 0. The behavior of a constant $G'(\omega)$ at $\omega \rightarrow 0$ is the sign of the formation of a gel plateau, according to the method by Nijenhuis and Winter.³⁵ Therefore, the liquid–solid transition could occur in the range of the value of the slope between near 0 and 1 for the $G'(\omega) \sim \omega$ curves or at a value of the slope between near 0 and 0.9 for the $G''(\omega) \sim \omega$ curves. Because $G'(\omega) \sim \omega^0$ or $G''(\omega) \sim \omega^0$ represented a gel state and $G'(\omega) \sim \omega^{0.9}$ or $G''(\omega) \sim \omega^{0.9}$ in the present work reflected homogeneous viscous liquid behavior. Figure 7a shows the concentration dependence of n' (exponent of $G'(\omega)$ to ω) and n'' (exponent of $G''(\omega)$ to ω) for PANI/cellulose solution at 25 °C. Both n' and n'' decreased with an increase of the cellulose concentration. The intersection took place at 3.8 wt % cellulose concentration (0.6 wt % PANI) with $n = n' = n''$ and $n = 0.74$, which can be defined as the gel point. Figure 7b shows $\tan \delta$ as a function of ω for the 0.6 wt % PANI/3.8 wt % cellulose aqueous solution. The $\tan \delta$ values hardly changed with various ω , supporting well the conclusion from Figure 7a. The cellulose in NaOH/thiourea aqueous solution exhibited an intersection value of the n' and n'' curves of 0.89,³⁷ which was larger than that of the PANI/cellulose solution. In general, the n value was related to the physically fractal dimension and reflected the degree of compactness of the network.^{38–40} A lower value of n indicated the formation of a more highly elastic

gel.^{41–43} The lower n value of the PANI/cellulose complex system suggested a more elastic network than the pure cellulose solution at the gel point. The results revealed that much stronger interactions between PANI and cellulose in the solution. The results also demonstrated that the Winter–Chambon criterion can be applied to describe the sol–gel transition of the PANI/cellulose complex solution.

The curves of G' and G'' for P15 PANI/cellulose solution over a period of 0–432 h at 8 °C are illustrated in Figure 8.

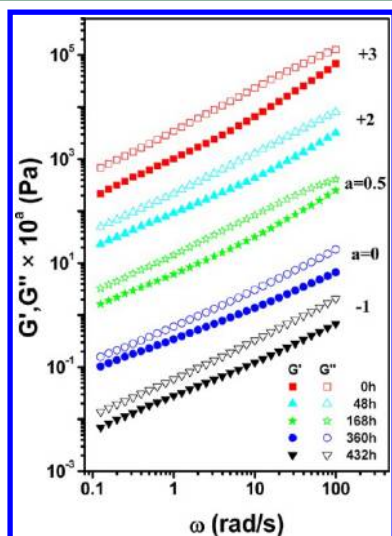


Figure 8. G' and G'' as a function of ω for the P15 PANI/cellulose solution at different storage times at 8 °C. The data are shifted along the vertical axis by 10^a to avoid overlapping.

During 0–360 h, G' was smaller than G'' in the full frequency range, indicating a liquidlike behavior. From our previous work, gel formation was found to take place in 4 wt % pure cellulose solution after 53 h at 8 °C.³¹ It was indicated that the supramolecular complexes constructed by the PANI and cellulose macromolecules were more stable than pure cellulose ICs. During 360–432 h, the value of G' was gradually getting closer to that of G'' in the terminal region, indicating the formation of a gel network. As mentioned above, the cellulose chains were entangled by PANI in the PANI/cellulose solution to construct a new complex composed of the hydrophobic PANI and the hydrophilic cellulose. The interaction between

the hydrophobic segments and the hydrophilic segments led to a more stable system than the cellulose solution, as a result of the reduction of the self-association of the hydrophilic cellulose chains. In the aqueous solutions, this method of the hydrophilic backbone incorporated with hydrophobic substituents gave rise to the formation and breakdown of the network, which were used to control rheology.^{44–50}

The crossover of G' and G'' curves can be used to determine the gel point for physically gelling systems,⁵¹ but the crossover point was dependent on frequency. Thus, the frequency of 1 rad/s was selected for all the samples. Figure 9a shows the temperature dependence of G' and G'' for the PANI/cellulose solution (see Table 1). Both G' and G'' exhibited the temperature dependence for all the samples. The G' and G'' values decreased slightly with increasing temperature in the beginning and then G'' was higher than G' , indicating a common viscoelastic behavior. Subsequently, in the vicinity of the crossover point, both G' and G'' were significantly increased and the value of G' was increasing much more rapidly, suggesting the partial formation of aggregates through hydrogen bonding. With increasing PANI content, the gel temperature first increased from 34 to 43 °C, and then decreased to 37 °C. The results indicated that, with a small amount of PANI, the existence of the hydrophobic PANI molecules entangled on the cellulose chains could stabilize the cellulose IC structure and counteracted the formation of the gel network. However, with a further increase of PANI, acidic phosphate ester doped PANI increased, which could break the inclusion complexes, resulting in the cellulose self-aggregation at lower temperature, leading to a decrease of the gelation temperature.

The temperature dependence of G' and G'' for the 0.6 wt % PANI/cellulose solution with different cellulose concentrations is shown in Figure 9b. The gelation temperature decreased with increasing cellulose concentration, which further confirmed that the gel was resulted from the self-association of cellulose chains through intermolecular hydrogen bonding. When the cellulose concentration was lower than 3 wt %, no gel point was observed, suggesting that the number of junction zones was not sufficient to form a continuous network. This was similar to the observation that the gelation temperature of the cellulose solution drops from 60.3 to 30.5 °C with the increasing of cellulose concentration from 3.0 to 5.0 wt % and that, when the cellulose concentration was below 3 wt %, no temperature-induced gelation behavior was observed.³¹ The results revealed further that cellulose concentration was the dominant factor in

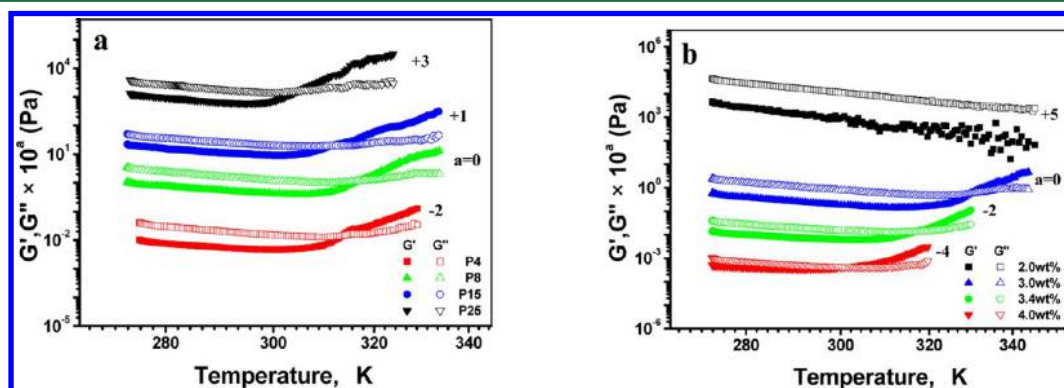


Figure 9. Temperature dependence of G' and G'' for P4, P8, P15, and P25 PANI/cellulose solutions (a) and temperature dependence of G' and G'' for the 0.6 wt % PANI/cellulose with concentrations from 2 to 4 wt % solutions (b). The data are shifted along the vertical axis by 10^a to avoid overlapping.

the formation of gels in the PANI/cellulose complex solution. The urea shell of the cellulose IC could be destroyed by increasing the temperature, leading to the physical cross-linking of cellulose.

The unique dependence of the gelation time on temperature for the P15 PANI/cellulose solution is illustrated in Figure 10.

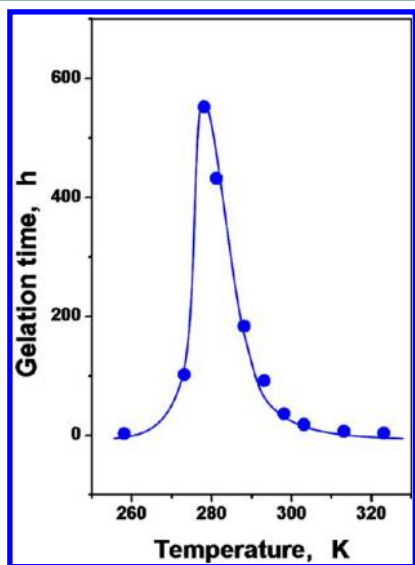


Figure 10. Gelation time as a function of temperature for the P15 PANI/cellulose solution.

The gelation time was indicated by the intersection of the G' and G'' curves for the PANI/cellulose solution at constant temperature. The gelation time dramatically increased from 2.3 h at $-10\text{ }^{\circ}\text{C}$ to a maximum of 552 h at $5\text{ }^{\circ}\text{C}$ and then reduced greatly to 36 h at $25\text{ }^{\circ}\text{C}$. The results revealed that either heating or cooling could induce gelation. However, the PANI/cellulose complex solution remained a liquid state for long time at the temperature range from 0 to $8\text{ }^{\circ}\text{C}$. This was very important for the both foundational research and industry process. These rheological properties were similar to those of the pure cellulose solution, indicating the gelation process was dominated by cellulose.³¹ The temperatures corresponding to gelation time shifted to higher temperatures by $5\text{ }^{\circ}\text{C}$ compared to the pure cellulose solution,³¹ further confirming that the PANI/cellulose complex reduced the self-association of the cellulose in the solution, leading to a more stable complex solution.

Figure 11 shows the gelation time (t_{gel}) dependence on temperature in the form of an Arrhenius plot for the PANI/cellulose solution. The activation energy (E_a) was calculated from the slope of the straight lines. Thus, we obtained the E_a values were 89.7 kJ/mol in the temperature range from 5 to $40\text{ }^{\circ}\text{C}$ and -150.7 kJ/mol from -10 to $5\text{ }^{\circ}\text{C}$, respectively. The activation energy is usually related to the interaction between macromolecules and chain conformation and can reflect the formation and rupture of linkages in “junction zones” during the gelation processes.⁵² The effects of temperature and molecular conformation on the gelation process may be reflected in the Arrhenius plot of $\ln(t_{\text{gel}})$ versus $1/T$.^{53,54} In the pure cellulose solution, the E_a value was 77.1 kJ/mol in the range from 0 to $30\text{ }^{\circ}\text{C}$ and -349.4 kJ/mol from -8 to $0\text{ }^{\circ}\text{C}$, respectively.³¹ The E_a value of the PANI/cellulose solution was higher than that of the pure cellulose solution in the

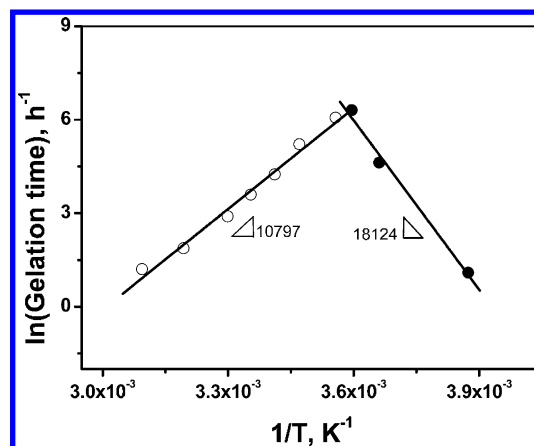


Figure 11. Arrhenius plots for the P15 PANI/cellulose solution. The number represents the slope of the line.

temperature range over $5\text{ }^{\circ}\text{C}$. The results suggested that the PANI/cellulose complexes displayed more stiffer chains than the pure cellulose. This was because both PANI and cellulose were stiff chains and, after the cellulose chains were entangled by PANI, the rigidity of the supramolecular complex chains were enhanced.^{31,55} The PANI/cellulose complex system exhibited a higher E_a value below $0\text{ }^{\circ}\text{C}$ than that above $5\text{ }^{\circ}\text{C}$, indicating the intermolecular interaction of PANI and cellulose at low temperature was much stronger than those among PANI and cellulose in the temperature higher than $5\text{ }^{\circ}\text{C}$. On the other hand, the E_a at below $0\text{ }^{\circ}\text{C}$ in the PANI/cellulose system was smaller than the pure cellulose solution, indicating weaker intermolecular interactions than in the pure cellulose networks.

Figure 12 shows the G' and G'' curves for the P15 PANI/cellulose solution under the heating–cooling process. In the

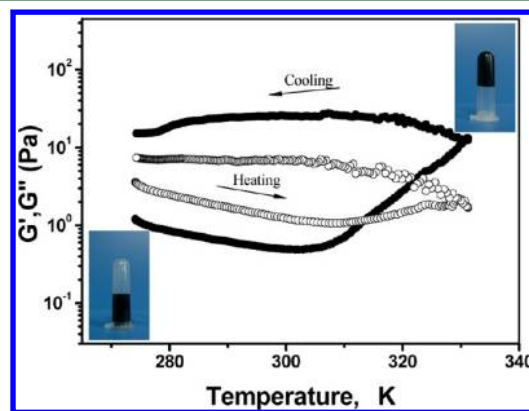


Figure 12. G' and G'' as a function of temperature in the heating and cooling processes for the P15 PANI/cellulose solution. Insets show the photographs of the P15 PANI/cellulose solution as liquid at $25\text{ }^{\circ}\text{C}$, as gels by heating at $50\text{ }^{\circ}\text{C}$.

heating process from 0 to about $50\text{ }^{\circ}\text{C}$, the crossover point of G' and G'' lied at $39.8\text{ }^{\circ}\text{C}$, and the curves were divided into three segments as follows. Below $30\text{ }^{\circ}\text{C}$, the G' values were lower than those of G'' and gradually decreased as the temperature increased, suggesting a typical viscoelastic behavior of a liquid. From 30 to $39.8\text{ }^{\circ}\text{C}$, the G'' values were slightly higher than those of G' . When the temperature was higher than $39.8\text{ }^{\circ}\text{C}$, both G' and G'' values increased sharply, and G' was higher than G'' , indicating an elastic gel network. To verify the

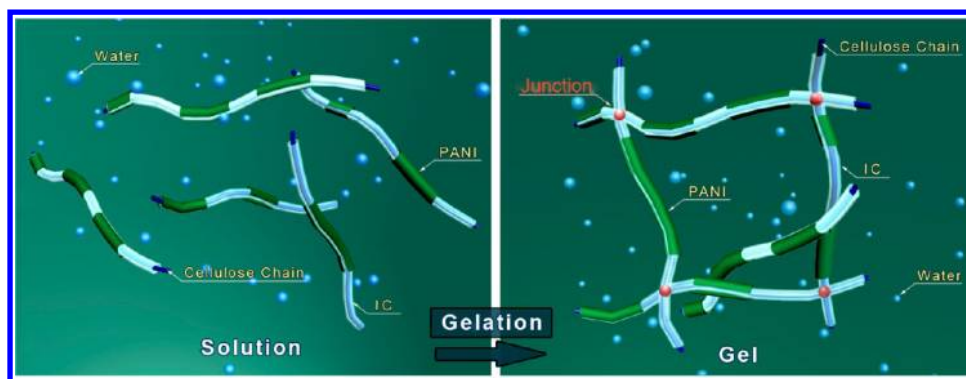


Figure 13. Schematic model to describe the sol–gel transition of PANI/cellulose solution.

thermoirreversibility of the sol–gel transition, the cooling process was started from 50 °C. In contrast to the G' and G'' curves obtained by heating, the cooling process showed different behaviors. The G' curve was always higher than the G'' curve in the whole temperature range, indicating a thermoirreversible behavior. This could be explained as follows. At higher temperatures, the urea shell of the cellulose IC was destroyed and the $-OH$ groups of the cellulose ICs was exposed to form hydrogen bonding association between cellulose chains. As a result, the PANI/cellulose supramolecular complex solution was changed to gels through the physical cross-linking and chains entanglement at elevated temperature. Moreover, the PANI/cellulose complex structure was formed under a certain condition at low temperature, and could not be reconstructed in this case as mentioned above, leading to the thermoirreversible property of the PANI/cellulose complex solution. The PANI/cellulose solution could form physical gels with a relatively high modulus across the whole temperature range. This phenomena was different, with a polymer solution at lower critical solution temperature, in which entropy-driven phase transition of the polymer produce precipitation occurred.⁵⁶ Thus, the PANI/cellulose gels were formed rather than becoming precipitate and suspension (Figure 12, inset).⁵⁷

Based on the evidence mentioned above, we proposed a schematic model to describe the sol–gel transition of PANI/cellulose solution as shown in Figure 13. In the complex solution, hydrophilic cellulose chains surrounded by urea have been entangled by hydrophobic PANI chains to form the homogeneous and stable solution in aqueous system (Figure 13a), supported by the TEM results in Figure 2 and G' and G'' data in Figures 4 and 8. At elevated temperature, the gel transition of PANI/cellulose complex solution occurred through the physical cross-linking and entanglement of the cellulose chains (Figure 13b), supported by the results in Figures 3, 9, and 12. The physical cross-linking junction formed easily on the cellulose IC with the exposure of $-OH$ groups through hydrogen bonding between cellulose chains.

CONCLUSION

A PANI/cellulose complex solution prepared in the cellulose/NaOH/urea aqueous system at low temperature represented a homogeneous liquidlike state. The PANI/cellulose supramolecular complex was constructed through the strong intermolecular hydrogen bonding between PANI and the cellulose ICs. The cellulose ICs were stable at low temperature, causing the water-soluble cellulose ICs surrounded by urea to be entangled by PANI to form the homogeneous solution in the PANI/cellulose mixture. The PANI/cellulose solution was

more stable than the pure cellulose solution, because PANI enhanced the stability of the complex solution. The cellulose concentration was the dominating factor in the gel formation. At elevated temperature, the cellulose IC structure was destroyed, and the exposed hydroxyl groups along the cellulose IC induced physical cross-linking and entanglement to give the gels. The PANI/cellulose solution exhibited a higher E_a value than that of the pure cellulose solution. The Winter–Chambon theory was proved to be applicable to describe the PANI/cellulose complex solution. The result revealed that the sol–gel transition of PANI/cellulose complex solution was thermoirreversible. Moreover, the PANI/cellulose complex solution could remain a liquid state for long time, showing good processability.

AUTHOR INFORMATION

Corresponding Author

*Phone: +86-27-87219274. Fax: +86-27-68762005. E-mail: lnzhang@public.wh.hb.cn.

Notes

The authors declare no competing financial interest.

ACKNOWLEDGMENTS

This work was supported by the National Basic Research Program of China (973 Program, 2010CB732203) and the National Natural Science Foundation of China (20874079).

REFERENCES

- (1) Huang, J.; Kaner, R. B. *J. Am. Chem. Soc.* **2004**, *126*, 851–855.
- (2) Yan, Y.; Yu, Z.; Huang, Y.; Yuan, W.; Wei, Z. *Adv. Mater.* **2007**, *19*, 3353–3357.
- (3) Kuila, B. K.; Nandan, B.; Bohme, M.; Janke, A.; Stamm, M. *Chem. Commun.* **2009**, *38*, 5749–5751.
- (4) Domingues, S. H.; Salvatierra, R. V.; Oliveira, M. M.; Zabin, A. J. G. *Chem. Commun.* **2011**, *47*, 2592–2594.
- (5) MacDiarmid, A. G. *Angew. Chem., Int. Ed.* **2001**, *40*, 2581–2590.
- (6) MacDiarmid, A. G. *Angew. Chem., Int. Ed.* **2001**, *113*, 2649–2659.
- (7) Shi, X.; Zhang, L.; Cai, J.; Cheng, G.; Zhang, H.; Li, J.; Wang, X. *Macromolecules* **2011**, *44*, 4565–4568.
- (8) Hurtado, P. I.; Berthier, L.; Kob, W. *Phys. Rev. Lett.* **2007**, *98*, 135503.
- (9) Weiss, R. A.; Zhao, H. Y. *J. Rheol.* **2009**, *53*, 191–213.
- (10) Meng, X. X.; Russel, W. B. *Macromolecules* **2005**, *38*, 593–600.
- (11) Kujawa, P.; Audibert-Hayet, A.; Selb, J.; Candau, F. *Macromolecules* **2006**, *39*, 384–392.
- (12) Tabuteau, H.; Ramos, L.; Nakaya-Yaegashi, K.; Imai, M.; Ligoure, C. *Langmuir* **2009**, *25*, 2467–2472.
- (13) Nakaya-Yaegashi, K.; Ramos, L.; Tabuteau, H.; Ligoure, C. *J. Rheol.* **2008**, *52*, 359–377.

- (14) Stadler, F. J.; Pyckhout-Hintzen, W.; Schumers, J. M.; Fustin, C. A.; Gohy, J. F.; Bailly, C. *Macromolecules* **2009**, *42*, 6181–6192.
- (15) Feldman, K. E.; Kade, M. J.; Meijer, E. W.; Hawker, C. J.; Kramer, E. J. *Macromolecules* **2009**, *42*, 9072–9081.
- (16) Binder, W. H.; Kunz, M. J.; Kluger, C.; Hayn, G.; Saf, R. *Macromolecules* **2004**, *37*, 1749–1759.
- (17) Adachi, K.; Irie, H.; Sato, T.; Uchibori, A.; Shiozawa, M.; Tezuka, Y. *Macromolecules* **2005**, *38*, 10210–10219.
- (18) Pickrahn, Katie.; Rajaram, B.; Mohraz, A. *Langmuir* **2010**, *26*, 2392–2400.
- (19) Helgeson, M. E.; Hodgdon, T. K.; Kaler, E. W.; Wagner, N. J. *Langmuir* **2010**, *26*, 8049–8060.
- (20) Chen, D. T. N.; Chen, K.; Hough, L. A.; Islam, M. F.; Yodh, A. G. *Macromolecules* **2010**, *43*, 2048–2053.
- (21) Ramakrishnan, S.; Zukoski, C. F. *Langmuir* **2006**, *22*, 7833–7842.
- (22) Herbst, F.; Schröter, K.; Gunkel, I.; Gröger, S.; Thurn-Albrecht, Th.; Balbach, J.; Binder, W. H. *Macromolecules* **2010**, *43*, 10006–10016.
- (23) Yang, Z.; Han, C. D. *Macromolecules* **2008**, *41*, 2104–2118.
- (24) Cai, J.; Liu, Y.; Zhang, L. *J. Polym. Sci., Part B: Polym. Phys.* **2006**, *44*, 3039–3101.
- (25) Zhang, H.; Wang, X.; Li, J.; Mo, Z.; Wang, F. *Polymer* **2009**, *50*, 2674–2679.
- (26) Luo, J.; Zhang, H.; Wang, X.; Li, J.; Wang, F. *Macromolecules* **2007**, *40*, 8132–8135.
- (27) Cai, J.; Zhang, L.; Liu, S. *Macromolecules* **2008**, *41*, 9345–9351.
- (28) Winter, H. H.; Chambon, F. J. *J. Rheol.* **1986**, *30*, 367–382.
- (29) Chambon, F. J.; Winter, H. H. *J. Rheol.* **1987**, *31*, 683–697.
- (30) Sharma, J.; Clarke, N. J. *Phys. Chem. B* **2004**, *108*, 13220–13230.
- (31) Cai, J.; Zhang, L. *Biomacromolecules* **2006**, *7*, 183–189.
- (32) Ferry, J. D. *Viscoelastic Properties of Polymers*, 3rd ed.; Wiley: New York, 1980.
- (33) Niu, Y. H.; Wang, Z. G. *Macromolecules* **2006**, *39*, 4175–4183.
- (34) Izuka, A.; Winter, H. H. *Macromolecules* **1994**, *27*, 6883–6888.
- (35) Nijenhuis, K.; Winter, H. H. *Macromolecules* **1989**, *22*, 411–414.
- (36) Lue, A.; Zhang, L. *Macromol. Biosci.* **2009**, *9*, 488–496.
- (37) Lue, A.; Zhang, L. *J. Phys. Chem. B* **2008**, *112*, 4488–4495.
- (38) Scanlan, J. C.; Winter, H. H. *Macromolecules* **1991**, *24*, 47–54.
- (39) Izuka, A.; Winter, H. H. *Macromolecules* **1992**, *25*, 2422–2428.
- (40) Madbouly, S. A.; Otaigbe, J. U. *Macromolecules* **2005**, *38*, 10178–10184.
- (41) Gao, S.; Nishinari, K. *Biomacromolecules* **2004**, *5*, 175–185.
- (42) Nordby, M. H.; Kjøniksen, A. L.; Nyström, B.; Roots, J. *Biomacromolecules* **2003**, *4*, 337–343.
- (43) Kjøniksen, A. L.; Hiorth, M.; Roots, J.; Nysrtom, B. *J. Phys. Chem. B* **2003**, *107*, 6324–6328.
- (44) Shaw, K. G.; Leipold, D. P. *J. Coat. Technol.* **1985**, *57*, 63–72.
- (45) Tanaka, R.; Meadows, J.; Williams, P. A.; Phillips, G. O. *Macromolecules* **1992**, *25*, 1304–1310.
- (46) Nystrom, B.; Thuresson, K.; Lindman, B. *Langmuir* **1995**, *11*, 1994–2002.
- (47) Castelletto, V.; Hamley, I. W.; Xue, W.; Sommer, C.; Pedersen, J. S.; Olmsted, P. D. *Macromolecules* **2004**, *37*, 1492–1501.
- (48) Piculell, L.; Egermayer, M.; Sjostrom, J. *Langmuir* **2003**, *19*, 3643–3649.
- (49) Thuresson, K.; Nilsson, S.; Kjoniksen, L.; Walderhaug, H.; Lindman, B.; Nystrom, B. *J. Phys. Chem. B* **1999**, *103*, 1425–1436.
- (50) Dreiss, C. A. *Soft Matter* **2007**, *3*, 956–970.
- (51) Li, L.; Aoki, Y. *Macromolecules* **1997**, *30*, 7835–7841.
- (52) Mitchell, J. R. *J. Text. Stud.* **1976**, *7*, 313–339.
- (53) Maekaji, K. *Agric. Biol. Chem.* **1973**, *37*, 2433–2434.
- (54) Huang, L.; Takahashi, R.; Kobayashi, S.; Kawase, T.; Nishinari, K. *Biomacromolecules* **2002**, *3*, 1296–1303.
- (55) Zhou, J.; Zhang, L.; Cai, J. *J. Polym. Sci., Polym. Phys.* **2004**, *42*, 347–353.
- (56) Eggenhuisen, T. M.; Becer, C. R.; Fijten, M. W. M.; Eckardt, R.; Hoogenboom, R.; Schubert, U. S. *Macromolecules* **2008**, *41*, 5132–5140.
- (57) Boudet, C.; Iliopoulos, I.; Poncelet, O.; Cloitre, M. *Biomacromolecules* **2005**, *6*, 3073–3078.